

## Article

# H-Beta Zeolite as Catalyst for the Conversion of Carbohydrates into 5-Hydroxymethylfurfural: The Role of Calcination Temperature

Xinyi Xing<sup>1,2</sup>, Wannu Liu<sup>2</sup>, Siquan Xu<sup>2</sup> and Jianxiu Hao<sup>1,2,\*</sup>

<sup>1</sup> School of Chemistry & Chemical Engineering, Suzhou University, Suzhou 234000, China; xingxinyi0206@163.com

<sup>2</sup> School of Forestry and Landscape Architecture, Anhui Agricultural University, Hefei 230031, China; liuwanni817@163.com (W.L.); siquanxu@ahau.edu.cn (S.X.)

\* Correspondence: haojx2021@ahszu.edu.cn

**Abstract:** H-Beta zeolite is a solid acid catalyst commonly utilized in the catalytic conversion of biomass resources. In this study, H-Beta zeolite was calcined at different temperatures (350, 550, 750, and 1000 °C) to explore the effects of high temperature-induced dealumination on its physicochemical properties and its catalytic ability to convert glucose into 5-hydroxymethylfurfural (HMF). It was shown that as the calcination temperature increased, the Si-O-Al bond of H-Beta zeolite was broken and its dealumination effect was enhanced. Dealumination led to the collapse of the framework of H-Beta zeolite and a reduction in the number of acid sites, which in turn reduced its catalytic performance and the efficiency of HMF formation from glucose. Furthermore, H-Beta zeolite exhibited an extraordinary catalytic ability for the production of HMF from carbohydrates. Using glucose and cellulose as substrates, superior HMF yields of 91% and 46%, respectively, were achieved under optimal reaction conditions. Further, calcination removes carbon deposits in the recovered H-Beta zeolite, but it affects the cycling stability of the catalyst. Meanwhile, the by-products formed during the synthesis of HMF from glucose catalyzed by H-Beta zeolite catalyst were also clearly detected.

**Keywords:** heterogeneous; 5-hydroxymethylfurfural; H-Beta; biomass; dealumination



**Citation:** Xing, X.; Liu, W.; Xu, S.; Hao, J. H-Beta Zeolite as Catalyst for the Conversion of Carbohydrates into 5-Hydroxymethylfurfural: The Role of Calcination Temperature. *Catalysts* **2024**, *14*, 248. <https://doi.org/10.3390/catal14040248>

Academic Editor: Narendra Kumar

Received: 24 February 2024

Revised: 15 March 2024

Accepted: 1 April 2024

Published: 8 April 2024



**Copyright:** © 2024 by the authors. Licensee MDPI, Basel, Switzerland. This article is an open access article distributed under the terms and conditions of the Creative Commons Attribution (CC BY) license (<https://creativecommons.org/licenses/by/4.0/>).

## 1. Introduction

Overexploitation of fossil fuels and growing environmental concerns have sparked a research upsurge in renewable resources. As a carbon-rich renewable resource, biomass is attracting close attention from academia and industry [1]. Numerous study efforts have focused on converting biomass into high value-added chemicals and biofuels. Among them, 5-hydroxymethylfurfural (HMF) has broad application pathways and can be used as a key intermediate in the synthesis of various serviceable polymer materials, plastic resins, and diesel additives in the chemical industry [1,2]. Fructose is easily dehydrated, and when used as a substrate, HMF can be obtained in high yield and selectivity [3,4]. However, the large-scale use of fructose to prepare HMF is impractical due to the shortage of natural reserves and its high cost and widespread use in the food and pharmaceutical industries. In addition, it is difficult to obtain satisfactory HMF yields from cellulose due to its robust structure and hydrolysis difficulties. Glucose, therefore, as an isomer of fructose, is regarded as the most suitable raw material for the preparation of HMF because of its reasonable price and abundant reserves [5].

The cascade pathway to yield HMF from glucose consists of two processes: (I) isomerization of glucose into fructose driven by Lewis acid assistance, and (II) dehydration of fructose to HMF under the catalysis of Brønsted acid [5,6]. Given the advantage of the absence of boundary phases, homogeneous catalysts such as organic acid [7], metal salt [8], and modified ionic liquids [9] have been widely employed and resulted in favourable HMF

yields from glucose. However, due to the objective challenges of difficult separation and recovery, reusable heterogeneous solid acid catalysts, such as zeolite [10], metal oxides [11], acidity resins [12], and acidic carbons [13], have recently become more popular. For heterogeneous catalysts, the main problem that needs to be addressed is usually the inability to provide a sufficient amount of acid sites or the inherent incongruity of the ratio of Lewis and Brønsted sites. Insufficient or incongruent acid sites can lead to inefficient two-step cascade reactions of isomerization and dehydration, which causes lower HMF yields [14]. Therefore, advances in solid acid catalysts with suitable acidic characteristics are crucial for converting glucose into HMF.

H-Beta zeolite contains tetravalent aluminum atoms in tetrahedral positions and is a well-known solid acid catalyst that possesses both Lewis and Brønsted acidity for catalytic cracking, alkylation, alkyl transfer reactions, petrochemical processes, and adsorption [15,16]. Moreover, the catalytic properties of H-Beta zeolite are also excellent during the isomerization of glucose. For example, Liu et al. [17] utilized H-Beta zeolite to catalyze glucose isomerization and achieved a fructose selectivity of 61.6% in the gamma-butyrolactone/H<sub>2</sub>O system at 100 °C. Xia et al. [18] used H-Beta zeolite to catalyze the isomerization of glucose and obtained a fructose selectivity of 32% in water at 130 °C.

Based on the remarkable isomerization catalytic activity of H-Beta zeolite, numerous efforts have been made to prepare Beta zeolite-based catalysts by internal/external framework modification and apply them to the conversion of glucose into HMF, including dealumination [10], isomorphic substitution [15], impregnation [19], and ion exchange [20]. Tatsumi et al. [10] prepared dealuminated Beta zeolite by steam treatment, which catalyzed glucose to achieve 78% conversion and 43% HMF yield at 180 °C for 2 h. Liu et al. [15] prepared Sn-Beta zeolite through isomorphous substitution, which catalyzed glucose to achieve a 42% HMF yield at 160 °C for 2.5 h. Xiao et al. [19] prepared a Cr/Beta zeolite catalyst by the impregnation method, which catalyzed glucose to achieve a 72% HMF yield at 150 °C for 90 min, while the glucose was almost completely converted. Xia et al. [20] prepared Fe/Beta zeolite catalyst by ion exchange, which catalyzed glucose to afford 95% conversion and 61% HMF yield at 120 °C for 90 min.

As a convenient modification of H-Beta zeolite, dealumination can be conducted by calcination, steam, and nitric acid treatment [21]. Calcination is a frequent treatment to modify the form of Al species (dealumination) present in the zeolite structure and thus adjust the zeolite's acidic properties. Previous studies have reported that calcination dealumination increases the catalytic activity of Beta zeolite [10,22,23]. There are reports in the literature on the effect of calcination and steam treatment on the structure of Al atoms in the framework and the acid properties of NH<sub>4</sub>-Beta [10]. The results showed a decline in Brønsted acidity and an increase in Lewis acidity in the calcined Beta zeolite, that is, calcination improved the acidic properties of the zeolite. It is of momentous importance to explore the effect of high-temperature calcination on the dealumination of H-Beta zeolite because during the progress of producing HMF, H-Beta zeolite-derived catalysts need to be repeatedly calcined for preparation or decarbonization regeneration. Nevertheless, not all Beta-type zeolites increase in acidity upon calcination. Besides, no previous studies have investigated the effect of calcination temperature on the structure and acidity of H-Beta zeolite, nor the conversion of cellulose to HMF using cheap and easily available H-Beta zeolites.

In our previous study [16], the H<sub>2</sub>O/tetrahydrofuran (THF) biphasic system was confirmed to facilitate HMF formation while also being inexpensive and recyclable. To sum up, in the present study, a series of dealuminated H-Beta zeolites were prepared after calcination at different temperatures (350, 550, 750, and 1000 °C), and the effect of calcination temperature on the structure and acidity of the H-Beta zeolites was analysed. Negative effects of calcination on zeolites were proposed and the reasons for the negative effects were investigated. Additionally, H-Beta zeolite was used as a catalyst to convert glucose and cellulose into HMF in an H<sub>2</sub>O/THF biphasic system. Further, the product of glucose

isomerization, fructose, was captured and the factors influencing glucose isomerization were analyzed.

## 2. Results and Discussion

### 2.1. Catalyst Characterization Analysis

Figure 1a summarizes the XRD patterns of the H-Beta zeolite catalysts. It shows that the diffraction curve of the dealuminated H-Beta zeolites is consistent with that of the parent H-Beta zeolite. This reflects the fact that the crystal structure of the catalyst was not significantly damaged by dealumination after calcination at high temperature and the BEA-type structure was still maintained with high crystallinity.

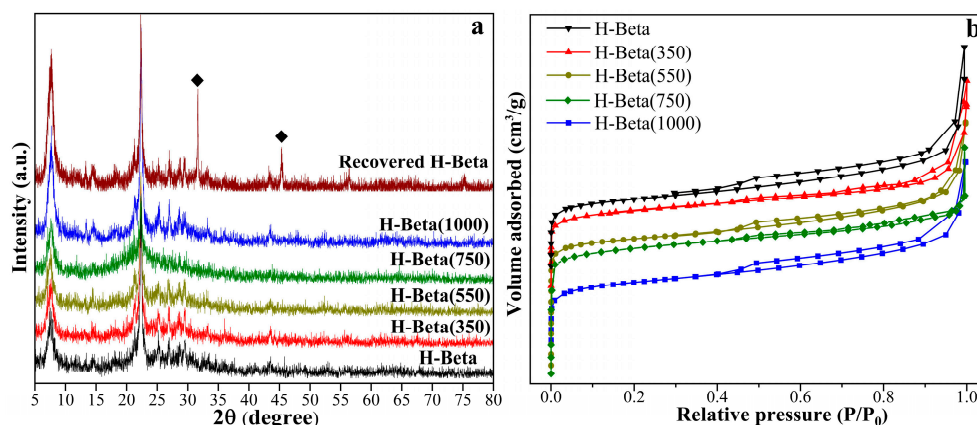


**Figure 1.** XRD patterns (a) and N<sub>2</sub> adsorption–desorption isotherms (b) of catalysts.

The N<sub>2</sub> adsorption–desorption isotherms of the H-Beta zeolites are listed in Figure 1b, and the texture properties are displayed in Table 1. As can be seen, all catalysts exhibit type IV isotherms with an H4 type hysteresis loop, which means that they are typical of microporous materials with the existence of mesopores [24]. Table 1 reflects that the specific surface area of the H-Beta zeolites declined (from 469 to 424 m<sup>2</sup>/g) while the pore volume increased (from 0.43 to 0.56 cm<sup>3</sup>/g) when the calcination temperature was increased to 550 °C. This is caused by the depletion of aluminum in the framework by dealumination, resulting in the reduction of micropores and the formation of more mesopores [25], which is also supported by the significantly increased mesopore volume (from 0.24 to 0.38 cm<sup>3</sup>/g). With the calcination temperature further increased to 1000 °C, the specific surface area (from 424 to 231 m<sup>2</sup>/g) and pore volume (from 0.56 to 0.30 cm<sup>3</sup>/g) of the catalyst decreased obviously. This is because an excessively severe calcination temperature breaks the Si-O-Al bonds of the parent H-Beta zeolite, resulting in a large-scale collapse of the framework [26].

**Table 1.** Physicochemical properties of catalysts.

Catalyst	SiO <sub>2</sub> /Al <sub>2</sub> O <sub>3</sub> <sup>a</sup> (mol)	S <sub>BET</sub> <sup>b</sup> (m <sup>2</sup> /g)	V <sub>pore</sub> <sup>c</sup> (cm <sup>3</sup> /g)	V <sub>meso</sub> <sup>d</sup> (cm <sup>3</sup> /g)	V <sub>micro</sub> <sup>e</sup> (cm <sup>3</sup> /g)	D <sub>mean</sub> <sup>f</sup> (nm)
H-Beta	30	469	0.43	0.24	0.19	3.66
H-Beta(350)	36	444	0.45	0.28	0.17	4.51
H-Beta(550)	50	424	0.56	0.38	0.18	5.31
H-Beta(750)	58	340	0.44	0.31	0.13	5.28
H-Beta(1000)	72	231	0.30	0.22	0.08	5.24
Recovered H-Beta	66	301	0.39	0.33	0.11	5.29

<sup>a</sup> Determined by ICP-AES. <sup>b</sup> BET surface area was determined from N<sub>2</sub> adsorption isotherm. <sup>c</sup> Volume of pore was determined from the single point desorption method. <sup>d</sup> Volume of mesopore = (V<sub>pore</sub> – V<sub>micro</sub>). <sup>e</sup> Volume of micropore was determined from the t-plot method. <sup>f</sup> Average pore size was determined from the desorption average pore diameter (4V/A by BET).

The SEM images (Figure 2) exhibit that all of the crystals of H-Beta zeolite have no significant differences in morphology or diameter before and after high-temperature dealumination (350 °C, 550 °C, 750 °C, and 1000 °C), indicating that high-temperature calcination has an inappreciable impact on the crystal structure of the H-Beta, which further corroborates the analysis results of the XRD.

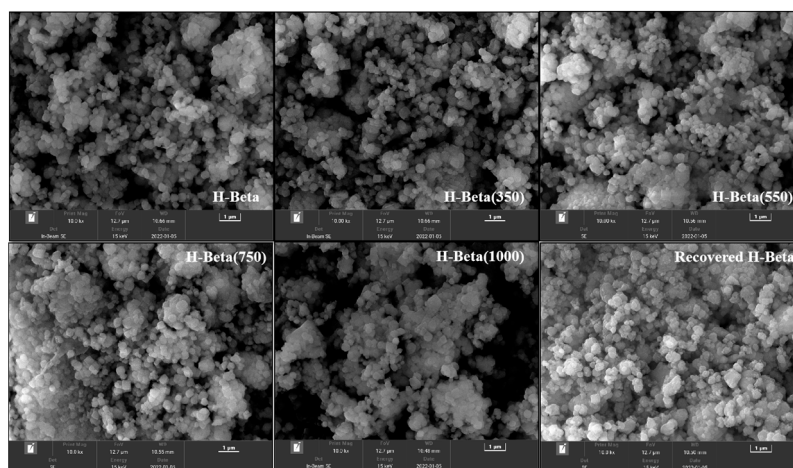


Figure 2. SEM images of catalysts.

550 °C is the usual calcination temperature for zeolites and at 1000 °C the structure is expected to be completely, or at least significantly, destroyed. Thus, the parent H-Beta zeolite, H-Beta(550), and H-Beta(1000) were selected for the  $^{27}\text{Al}$  MAS NMR testing, as shown in Figure 3. It can be clearly seen that at 53 and 0 ppm, obvious peaks appear in all catalysts, which are attributed to aluminium species in the tetrahedral environment ( $\text{AlO}_4$ ) in the framework and aluminium species in the extra-framework octahedral environment ( $\text{AlO}_6$ ), respectively [27,28]. The relative intensities of two types of aluminium species were calculated to measure the proportion of the aluminium species in the catalysts: H-Beta ( $\text{AlO}_4$ : 88%,  $\text{AlO}_6$ : 12%), H-Beta(550) ( $\text{AlO}_4$ : 81%,  $\text{AlO}_6$ : 19%), and H-Beta(1000) ( $\text{AlO}_4$ : 76%,  $\text{AlO}_6$ : 24%), respectively. This demonstrates the fact that as the calcination temperature increases, the dealumination effect of H-Beta zeolite is gradually enhanced, and more aluminium in the framework is depleted. Furthermore, H-Beta zeolite has peak areas greater than H-Beta(550) and H-Beta(1000) at 50 and 0 ppm, indicating the depletion of Al species during calcining, which confirms the ICP-AES results (Table 1).

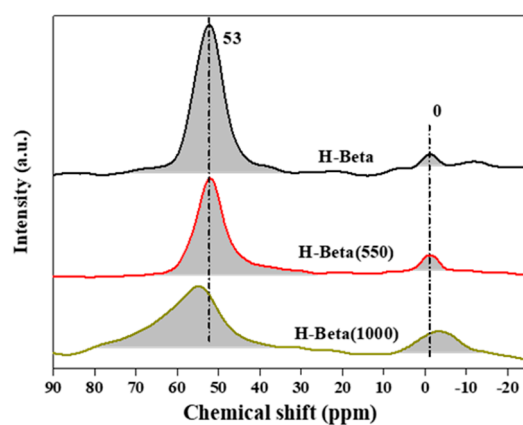
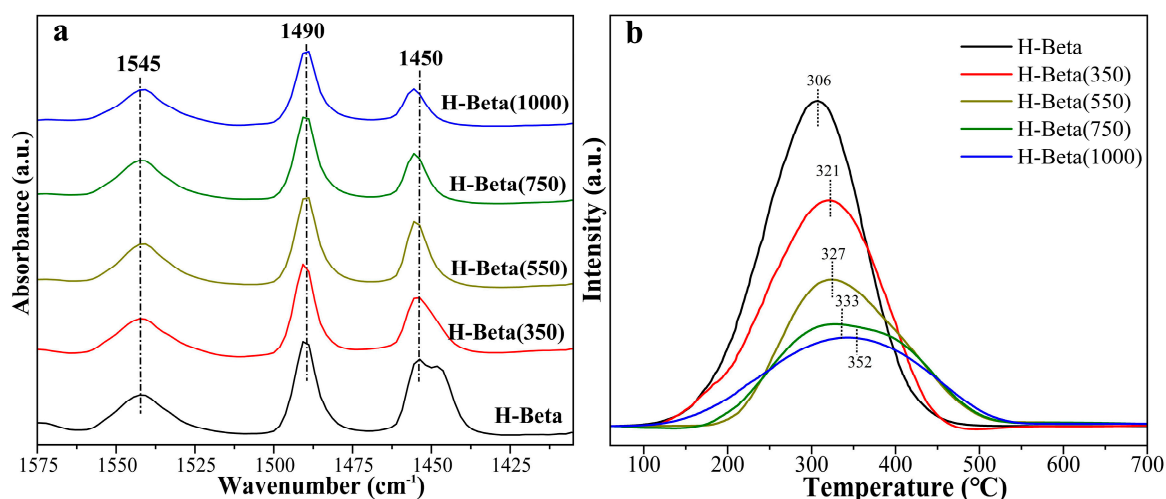


Figure 3.  $^{27}\text{Al}$  MAS NMR spectra of catalysts.

The dealumination caused by calcination mainly affects the framework structure of the H-Beta zeolite, which in turn results in a change of its acidic characteristics. Therefore, Py-FTIR and  $\text{NH}_3$ -TPD were used simultaneously to analyse the concentration and strength of

acid sites in the catalysts in detail. As can be seen from the Py-FTIR analysis in Figure 4a, all catalysts clearly exhibit three bands. The peaks around 1450 and 1545  $\text{cm}^{-1}$  are assigned to Lewis acid and Brønsted acid sites, respectively, and meanwhile, the peak around 1490  $\text{cm}^{-1}$  belongs to both Lewis and Brønsted acid sites [29]. The acidity of the H-Beta zeolite is listed in Table 2. It can be seen that with the increase of the calcination temperature, the Lewis acid, Brønsted acid, and total acidity of the H-Beta zeolite all dropped sharply. This phenomenon is caused by the depletion of extra-framework and framework aluminium due to enhanced dealumination, which is also confirmed by the increasing Si/Al ratio from ICP-AES (Table 1). It is worthwhile noting that the number of Brønsted acid sites is expected to decrease less than the number of Lewis acid sites with the increase in calcination temperature. Obviously, this depends on the degree of damage of the structure. Even though some of the Brønsted acid is converted to Lewis acid during the calcination process, extra-framework aluminium (Lewis acidity) is more easily destroyed during the calcination process than framework aluminium (Brønsted acidity), which is consistent with a previous study [30].



**Figure 4.** (a) Py-FTIR spectra and (b)  $\text{NH}_3$ -TPD profiles of catalysts.

**Table 2.** Acidity of catalysts <sup>a</sup>.

Catalyst	Lewis Acid Sites ( $\mu\text{mol/g}$ )	Brønsted Acid Sites ( $\mu\text{mol/g}$ )	Total Acidity ( $\mu\text{mol/g}$ )	Ratio of Lewis to Brønsted Site
H-Beta	259	232	491	1.12
H-Beta(350)	228	225	453	1.01
H-Beta(550)	153	222	375	0.69
H-Beta(750)	90	213	303	0.42
H-Beta(1000)	70	192	262	0.36
Recovered H-Beta	99	190	289	0.52

<sup>a</sup> Determined by Py-FTIR at 150 °C.

The  $\text{NH}_3$ -TPD profiles in Figure 4b clearly show that the desorption peaks of all catalysts appear within the scope of 300–500 °C belonging to the moderate acid sites [31], which means that in the H-Beta zeolite before and after dealumination, the active sites are all moderate acid sites. Interestingly, the desorption temperatures of the  $\text{NH}_3$  desorption peaks of dealuminated H-Beta zeolites gradually increased compared to the parent H-Beta zeolite, demonstrating the increased acid strength. This consequence is reasonable as the residual aluminium species in H-Beta zeolite would be more isolated, resulting in the generation of stronger acidic isolated Si-O-Al bonds, which is also the source of acidity of the H-Beta zeolite [29].

## 2.2. The Production of HMF from Glucose

So as to uncover the effect of the calcination-induced dealumination of H-Beta zeolite on its catalytic properties, the catalytic activity of the H-Beta zeolites on the conversion of glucose into HMF at different temperatures (140–180 °C) was studied in detail. As shown in Figure 5, as the calcination temperature increased, the corresponding H-Beta and the dealuminated H-Beta zeolite catalysts exhibited a significant decrease in activity sequentially. Under their respective optimal reaction conditions, the best HMF yields achieved by the H-Beta, H-Beta(550), and H-Beta(1000) catalysts were 91%, 84%, and 61%, respectively. The reason why the catalytic activity decreases sequentially is due to the enhanced dealumination and the significant reduction of acid sites, resulting in insufficient active sites of the catalyst. In addition, the decrease in the ratio between Lewis to Brønsted acidity caused by dealumination is also responsible. The production of HMF from glucose is a cascade step catalysed by Lewis and Brønsted acidity, so there is an optimal dynamic equilibrium [6,32]. Lower Lewis to Brønsted acid site ratios do not favour the formation of intermediate fructose, which is a crucial rate-limiting step, so the HMF yields achieved are lower. These results reflect the fact that for H-Beta zeolite, the dealumination effect brought by calcination will lead to a significant loss of its acidic active sites, which is not conducive to converting the glucose into HMF.

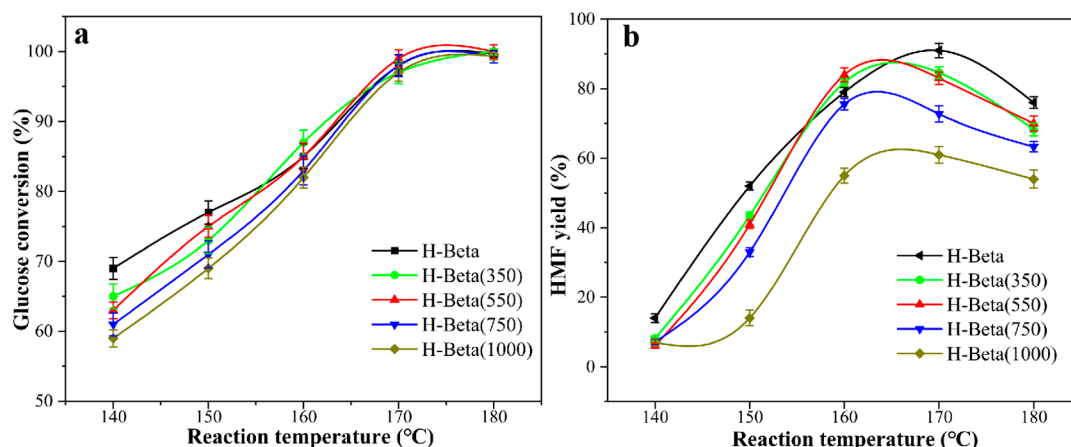


**Figure 5.** Performance comparison of H-Beta and calcined Beta zeolite catalysts on (a) glucose conversion and (b) HMF yield. Reaction condition: glucose (100 mg), catalyst (30 mg), NaCl (20 mg), H<sub>2</sub>O (1 mL), THF (4 mL), reaction time (2 h).

After confirming the superior performance of H-Beta zeolite catalyst, a detailed screening of reaction conditions, starting from the reaction temperature and reaction time, was employed to make further breakthroughs in HMF yields. As observed in Figure 6, the reaction temperature and reaction time play vital roles in the progress of HMF production. The resulting glucose conversion (17%) and HMF yield (4%) were poor at 140 °C for 1 h. As the reaction temperature and time increased, the conversion of glucose and the yield of HMF were greatly improved, and a distinguished HMF yield (91%) was acquired at 170 °C for 2 h. This result implies that sufficient system energy is necessary to achieve high HMF yields, which is beneficial for the acceleration of the reaction rate. However, the excessively severe hydrothermal environment not only promoted the conversion of glucose, but also accelerated the production of by-products [33]. For example, if the temperature or time was further increased from 170 °C for 2 h, the yield of HMF decreased. This is also verified by the organic phase, which is continuously browning after the reaction, and the recovered catalyst, which means the production of unwanted humins.

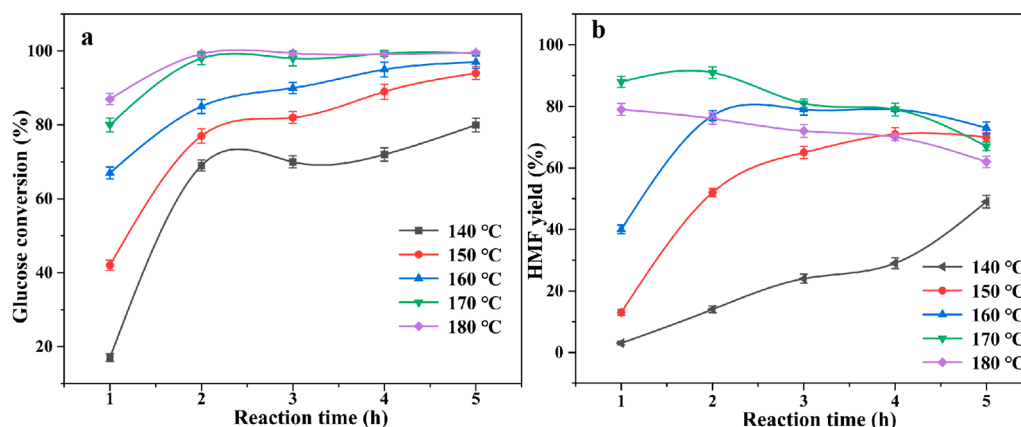


**Figure 6.** Effects of reaction temperature and reaction time on (a) glucose conversion and (b) HMF yield. Reaction condition: glucose (100 mg), catalyst (30 mg), NaCl (20 mg), H<sub>2</sub>O (1 mL), THF (4 mL).

The effect of H-Beta catalyst dosage on HMF production from glucose was explored and is exhibited in Figure 7. Clearly, in the blank contrast group, only a low level of 15% HMF yield was achieved. The necessary activation energy for the reaction was reduced as H-Beta zeolite was employed as a catalyst. With the increase of the catalyst dosage, the corresponding HMF yield and glucose conversion were also gradually enhanced. The best HMF yield of 91% was achieved at 30 mg, and the glucose was almost completely converted. It is suggested that high acid density helps to accelerate glucose conversion while enhancing HMF yield. However, as a further enhancement of the catalyst dosage to 40 and 50 mg, the yield of HMF was limited. These results indicate that sufficient active sites in the catalytic system are necessary to give the anticipated HMF yield; nonetheless, excess useful sites result in yield-loss reactions, which reduce the HMF yield [34].

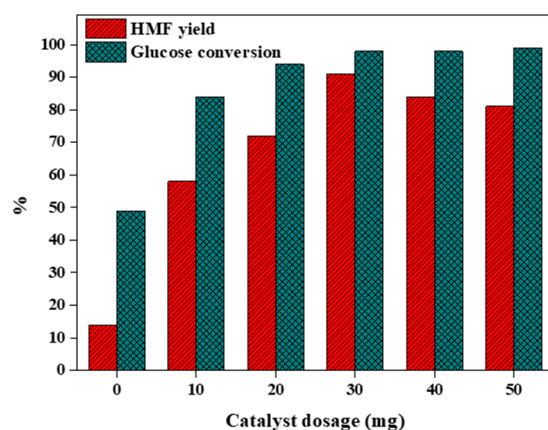


**Figure 7.** Effects of catalyst dosage on H-Beta-catalysed glucose conversion. Reaction condition: glucose (100 mg), NaCl (20 mg), H<sub>2</sub>O (1 mL), THF (4 mL), reaction temperature (170 °C), reaction time (2 h).

From an industrial point of view, high substrate concentrations are desirable in view of cost constraints. As shown in Figure 8, the effect of initial glucose loading on the HMF yield was performed in the range of 50 to 250 mg. The HMF yield achieved when the glucose concentration was set to 50 mg (71%) was low compared to 100 mg (91%) due to the fact that the catalyst density was too high to promote the occurrence of side reactions. Remarkably, when the glucose loading was further increased to 150 (80%), 200 (67%), or even 250 mg (58%), the obtained HMF yields were still considerable, indicating the superior performance of this catalytic system. This result demonstrates that for the synthesis of HMF from glucose, the yield-loss reaction is more likely to occur in a system

environment with a high substrate concentration. For the yield loss-reaction of HMF, two routes are recognized, that is, (1) HMF is rehydrated to form formic acid and levulinic acid; and (2) HMF undergoes condensation polymerization with other organic molecules or intermediates in the system to form humins and soluble by-products [35].

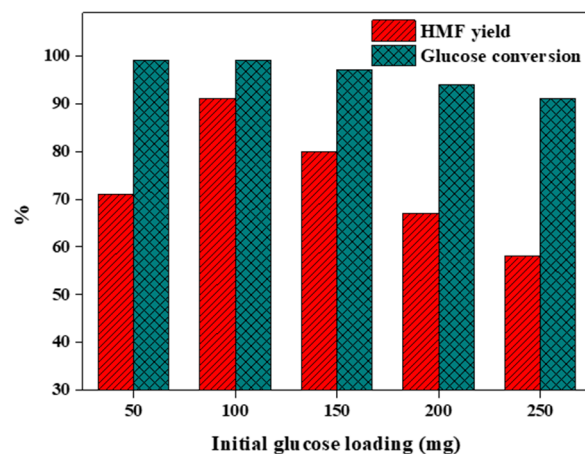


**Figure 8.** Effects of initial glucose loading on HMF yield. Reaction condition: H-Beta zeolite catalyst (30 mg), NaCl (20 mg), H<sub>2</sub>O (1 mL), THF (4 mL), reaction temperature (170 °C), reaction time (2 h).

The reaction solvent is also a crucial element in the catalytic synthesis of HMF, as it not only regulates the dispersion and conversion of substrate, but also affects the species and degradation of products, reaction networks, and activation energies [36]. The catalytic properties of the same catalyst in different solvent systems may be different. Herein, the synthesis of HMF from glucose using H-Beta zeolite as a catalyst exhibited high efficiency in H<sub>2</sub>O/THF, so the impact of different component ratios on the HMF yield was explored. Figure 9 describes an optimal volume ratio between the aqueous phase and the THF phase (organic phase). The aqueous phase is used as the occurrence phase of the catalytic reaction, and its excess will increase the likelihood of HMF rehydration. The THF phase is used as the extraction phase, and its excess will increase the formation potential of humins [37,38]. After screening, it was determined that during the conversion of H-Beta zeolite-catalysed glucose to HMF in the H<sub>2</sub>O/THF biphasic system, the optimal volume ratio of THF to H<sub>2</sub>O was 4:1 (mL/mL).

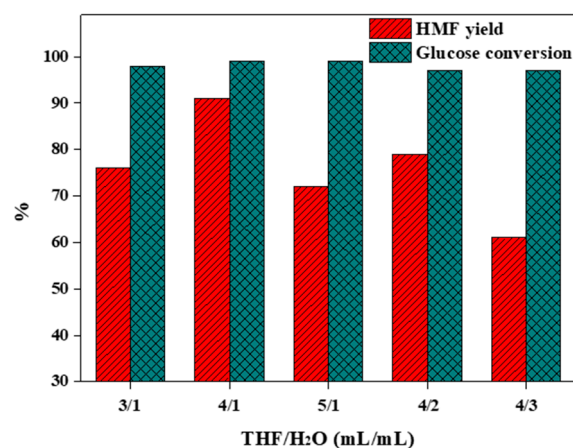


**Figure 9.** Effects of system component ratio on HMF yield. Reaction condition: glucose (100 mg), H-Beta zeolite catalyst (30 mg), NaCl (20 mg), reaction temperature (170 °C), reaction time (2 h).

### 2.3. Production of Fructose from Glucose

The isomerization of glucose into fructose is the rate-limiting step in the synthesis of HMF and it is clearly catalysed by Lewis acids [32]. To further elucidate the effect of H-Beta zeolite on this step after calcination dealumination, H-Beta zeolite catalysts were tested to catalyse the isomerization of fructose from glucose in an aqueous phase. As summarized in Table S1, the best fructose selectivities achieved for the H-Beta, H-Beta(350), H-Beta(550), H-Beta(750), and H-Beta(1000) catalysts were 29%, 24%, 19%, 15%, and 11%, respectively. Apparently, their catalytic properties in catalysing the isomerization of glucose exhibit a clear correlation with Lewis acidity. Moreover, because the Lewis acidity of the three decreased significantly (259  $\mu\text{mol/g}$ , 228  $\mu\text{mol/g}$ , 153  $\mu\text{mol/g}$ , 90  $\mu\text{mol/g}$ , and 70  $\mu\text{mol/g}$  in sequence), the Brønsted acidity decreased relatively gently (232  $\mu\text{mol/g}$ , 225  $\mu\text{mol/g}$ , 222  $\mu\text{mol/g}$ , 213  $\mu\text{mol/g}$ , and 192  $\mu\text{mol/g}$  in sequence). Therefore, it can be reasonably determined that the differences in the catalytic properties of the H-Beta, H-Beta(350), H-Beta(550), H-Beta(750), and H-Beta(1000) zeolites in catalysing the synthesis of HMF from glucose mainly depends on the change of Lewis acidity. A high Lewis acidity is beneficial to accelerate the isomerization of glucose and thus contribute to the formation of HMF, which further supports the previous analysis results of the Lewis to Brønsted acid site ratios.

### 2.4. By-Products Formed during the Reaction

In addition to the directly observable humins, soluble by-products produced in the H-Beta zeolite-catalysed glucose-to-HMF reaction were identified by GC-MS. As can be seen from Figure S1, there is another important platform compound, furfural, which is present at a negligible concentration, along with the formation of the target product HMF. A similar phenomenon has been reported in the literature [39] and the reason is that in the presence of a Lewis acid site, a small amount of fructose undergoes a retro-aldol reaction to generate xylose, which can be dehydrated to form furfural. The detected soluble by-products also include C3-C26 molecules of uncertain structure, which are due to fragmentation of HMF, or side reactions such as esterification, condensation, and polymerization with other molecules [34]. It is worth noting that levulinic acid was not detected as a hydration product of HMF, because the acid sites on the H-Beta zeolite surface were not strong enough to drive HMF to continue the rehydration reaction. This behaviour was also previously observed by Carlini et al. [40].

### 2.5. Synthesis of HMF from Cellulose

For the transformation of glucose to fructose as well as HMF, H-Beta zeolite exhibited a desired catalytic ability in the catalytic system chosen in this study. Immediately, its catalytic activity towards cellulose was also attempted. It is recognized that cellulose with glucose as a structural monomer is in a crystalline state and is difficult to hydrolyze. Consequently, the HMF yields typically achieved using it as a substrate are low. Table 3 shows that under various reaction conditions, the HMF yields achieved by H-Beta zeolite-catalysed cellulose conversion range from 16% to 46%. Among them, the optimal HMF yield of 46% was acquired at 200 °C for 6 h, which is remarkable. In addition, trace amounts of furfural as a by-product were also detected in the process.

**Table 3.** Conversion of cellulose to HMF catalysed by H-Beta zeolite.

Reaction Temperature (°C)	Reaction Time (h)	Cellulose Loading (mg)	HMF Yield (%)	Furfural Yield (%)
190	6	300	33	3
200	6	300	40	3
210	6	300	25	2
200	5	300	26	3
200	7	300	16	3
200	6	400	46	4
200	6	500	44	4

## 2.6. Catalyst Recycling Capacity

The above analysis of physicochemical properties demonstrates a result that the dealumination caused by high-temperature calcination will cause the H-Beta zeolite framework to collapse and the number of acid sites to decrease. In the process of solid acid-catalysed synthesis of HMF from glucose, if the catalyst needs to be recycled many times, a step of calcination to remove carbon deposits in the recovery process is essential. Therefore, in this study, we centrifuged, washed, filtered, and calcined (550 °C) the reacted H-Beta zeolite to remove carbon deposits, and then put it into the next use to observe its recycling ability. As shown in Figure 10, the H-Beta zeolite after two and multiple cycles showed a very pronounced trend of performance degradation compared to fresh, and the achieved yield level was nearly halved. To explore the reasons for the significant drop in the properties of H-Beta zeolite catalyst, the catalyst recovered by calcination to remove carbon deposits was characterized in detail. It can be clearly seen from Tables 1 and 2 that the collapsed framework of the catalyst under severe hydrothermal conditions and after the calcination step leads to a decline in the specific surface area and pore volume, while both Lewis-acid and Brønsted-acid sites were significantly reduced. Hence, it can be concluded that the reduction of active sites due to the framework collapse phenomenon of H-Beta zeolite during cycling is responsible for the drop in its catalytic property.

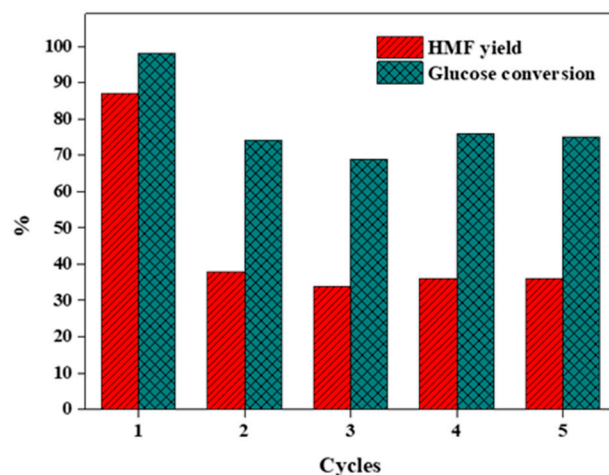


**Figure 10.** Evaluation of the cyclability of H-Beta zeolite catalyst. Reaction condition: glucose (100 mg), H-Beta zeolite catalyst (30 mg), NaCl (20 mg), reaction H<sub>2</sub>O (1 mL), THF (4 mL), temperature (170 °C), reaction time (2 h).

## 3. Materials and Methods

### 3.1. Materials and Catalyst Preparation

5-Hydroxymethylfurfural standard (>99%), furfural standard, D-(+)-glucose, sodium chloride (NaCl, 99.5%), and tetrahydrofuran (THF, >99.5%) were purchased from Aladdin Biochemical Technology Co., Ltd. (Shanghai, China). Microcrystalline cellulose was purchased from Thermo Scientific Chemicals Co., Ltd. (Beijing, China). Beta zeolite (SiO<sub>2</sub>/Al<sub>2</sub>O<sub>3</sub> = 30) was purchased from Nankai University Catalyst Factory (Tianjin, China). The cation type of the zeolite is hydrogen (H) and the Na<sub>2</sub>O content of the zeolite is 0.04%. All chemicals and materials were of analytical grade and were not further purified.

The dealuminated H-Beta zeolite samples were obtained by simple high-temperature calcination. Typically, 2.0 g of H-Beta zeolite was calcined in a tubular furnace at 550 °C for 2 h under an air atmosphere. The heating rate was 10 °C/min and the air flow rate was 50 mL/min. The obtained sample was denoted as H-Beta(550). The preparation process of the H-Beta(1000) sample was consistent with the above except that the calcination temperature was adjusted.

### 3.2. Catalyst Characterization

The content of Si and Al elements in the H-Beta zeolites was determined by ICP-AES (Perkin OPTIMA 5300DV, Philadelphia, PA, USA). The pore structure of the H-Beta zeolites was analysed by the N<sub>2</sub> adsorption–desorption method, which was performed on an ASAP 2460 gas sorption system (Micromeritics Instrument Co., Ltd., Shanghai, China). The structural characteristics of the samples were recorded by wide-angle powder X-ray diffraction (XD-3, 2θ = 5–80°, Ni-filtered Cu-Kα radiation, Beijing PERSEE, China). The morphology of the samples was identified using Inspect F50 electron microscopy (FEI, Pittsburgh, PA, USA). <sup>27</sup>Al solid-state NMR spectra of the samples were determined on a JEOL ECA-600 spectrometer (Peabody, MA, USA) (resonance frequency: 156.4 MHz, spinning rate: 15 kHz). The formation of by-products was determined by GC-MS (Gas Chromatograph: 7890B; Mass Spectrometer: 7000B, Agilent, Santa Clara, CA, USA).

The acidic strength of the samples was identified by NH<sub>3</sub>-temperature-programmed desorption (NH<sub>3</sub>-TPD, Micromeritics Autochem 2910, Micromeritics, Shanghai, China) equipped with a thermal conductivity detector (TCD). The samples were first treated with helium (He) gas at 500 °C for 2 h. Later, the samples were cooled to 50 °C in a He gas atmosphere, injected with NH<sub>3</sub> until the samples were saturated, and purged with He gas for a further 30 min to remove NH<sub>3</sub> from the sample surface. The amount of NH<sub>3</sub> adsorbed was measured by TCD. The NH<sub>3</sub>-TPD analysis proceeded from 50 °C to 700 °C at a rate of 10 °C/min in a He gas stream.

Pyridine adsorption infrared spectroscopy (Py-FTIR, Nicolet iS50, Thermo Fisher Scientific, Waltham, MA, USA) analysis was performed on a Frontier Fourier Transform Infrared Instrument. The samples were purged under vacuum (1 × 10<sup>−3</sup> Pa) for 2 h. After adsorption of pyridine at room temperature, the program was ramped up to the measurement temperature (150 °C) for vacuum desorption (1 × 10<sup>−3</sup> Pa) for 30 min, after which the samples were cooled to room temperature and the IR spectra were recorded in the 1700–1400 cm<sup>−1</sup> wavelength region.

### 3.3. Typical Procedure and Product Analysis

The synthesis of HMF from glucose and cellulose catalysed by dealumination H-Beta zeolite was conducted in a thick-walled pressure-resistant tube and a reaction still (NSG, Anhui Chem-n Instrument Co., Ltd., Hefei, China). In a typical experimental procedure, glucose (100 mg), catalyst (30 mg), and NaCl (200 mg) were sequentially added to a biphasic system consisting of THF (4.0 mL) and H<sub>2</sub>O (1.0 mL). Subsequently, the reactor was immersed in an oil bath and heated to 170 °C for 2 h with stirring (350 rpm). After the reaction was accomplished, the reactor was cooled to room temperature with cooling water, after which the products were separated by centrifugation. For the recovery experiment, after the solid catalyst was separated, it was washed with deionized water and absolute ethyl alcohol, and dried for further use.

HMF dissolved in the organic and aqueous phases was quantified using a high-performance liquid chromatograph (HPLC, Agres 1100, Dalian Elite Analytical Instruments Co., Ltd., Dalian, China) equipped with a C18 column (Supersil ODS2, Dalian Elite Analytical Instruments Co., Ltd.) and a UV detector (D1100) at 280 nm. The mobile phase was a mixed solution of methanol and water (7:3, v/v). The remaining glucose in the aqueous phase was measured by HPLC (Agilent 1200) equipped with a column (Agilent Hi-Plex H) and a Refractive Index detector, and the deionized water was used as a mobile phase. The Eqs. used in the study are listed below:

$$\text{Glucose conversion (mol \%)} = \frac{\text{moles of glucose reacted}}{\text{moles of glucose}} \times 100 \quad (1)$$

$$\text{HMF yield from glucose (mol \%)} = \frac{\text{moles of HMF produced}}{\text{moles of glucose}} \times 100 \quad (2)$$

$$\text{HMF yield from cellulose (mol \%)} = \frac{\text{moles of HMF produced}}{\text{moles of glucose unit in cellulose}} \times 100 \quad (3)$$

$$\text{HMF selectivity from glucose (mol \%)} = \frac{\text{moles of HMF produced}}{\text{moles of glucose reacted}} \times 100 \quad (4)$$

#### 4. Conclusions

Here, the effects of different calcination temperatures on the dealumination of H-Beta zeolite were investigated in detail. The results showed that an increase of calcination temperature enhanced the dealumination effect of H-Beta zeolite, which in turn led to the collapse of its framework and a reduction of the number of acid sites. Compared with dealuminated H-Beta zeolites, the reason for the desirable catalytic properties of H-Beta zeolite for the synthesis of HMF from glucose is due to its sufficient active sites, which are beneficial to accelerate the production of fructose, an important intermediate. Using H-Beta zeolite as a catalyst, optimal HMF yields of 91% and 46% were achieved from glucose and cellulose, respectively, after screening the reaction conditions. By-products formed during the catalytic process were identified as humins, furfural, and C<sub>3</sub>-C<sub>26</sub> organic molecules.

**Supplementary Materials:** The following supporting information can be downloaded at: <https://www.mdpi.com/article/10.3390/catal14040248/s1>, Table S1: Performance comparison of catalysts for the isomerization of glucose to fructose; Figure S1: GC-MS analysis of the THF phase recovered after the reaction.

**Author Contributions:** Investigation, Data curation, X.X.; Software, W.L.; Writing—original draft, S.X.; Writing—review and editing, Supervision, Funding acquisition, J.H. All authors have read and agreed to the published version of the manuscript.

**Funding:** This research was funded by the Suzhou University scientific research platform open project (2022ykf06); Anhui Province Higher Education Research Program Project (2023AH052225); Suzhou University doctoral research start-up fund project (2021BSK035).

**Data Availability Statement:** The data supporting this study are available when reasonably requested from the corresponding author.

**Conflicts of Interest:** The authors declare that they have no known competing financial interests or personal relationships that could appear to influence the work reported in this paper.

#### References

1. Mittal, A.; Pilath, H.M.; Johnson, D.K. Direct conversion of biomass carbohydrates to platform chemicals: 5-hydroxymethylfurfural (HMF) and furfural. *Energ. Fuel* **2020**, *34*, 3284–3293. [CrossRef]
2. Ling, R.; Wei, W.; Jin, Y. Pretreatment of sugarcane bagasse with acid catalyzed ethylene glycol-water to improve the cellulose enzymatic conversion. *Bioresour. Technol.* **2022**, *361*, 127723. [CrossRef]
3. Patil, C.R.; Rode, C.V. Synthesis of diesel additives from fructose over PWA/SBA-15 catalyst. *Fuel* **2018**, *217*, 38–44. [CrossRef]
4. Wang, L.; Zhang, L.; Li, H.; Ma, Y.; Zhang, R. High selective production of 5-hydroxymethylfurfural from fructose by sulfonic acid functionalized SBA-15 catalyst. *Compos. Part B-Eng.* **2019**, *156*, 88–94. [CrossRef]
5. Swift, T.D.; Nguyen, H.; Anderko, A.; Nikolakis, V.; Vlachos, D.G. Tandem Lewis/Brønsted homogeneous acid catalysis: Conversion of glucose to 5-hydroxymethylfurfural in an aqueous chromium (III) chloride and hydrochloric acid solution. *Green Chem.* **2015**, *17*, 4725–4735. [CrossRef]
6. Li, X.; Peng, K.; Liu, X.; Xia, Q.; Wang, Y. Comprehensive understanding of the role of Brønsted and Lewis acid sites in glucose conversion into 5-hydroxymethylfurfural. *ChemCatChem* **2017**, *9*, 2739–2746. [CrossRef]
7. Slak, J.; Pomeroy, B.; Kostyniuk, A.; Grilc, M.; Likozar, B. A review of bio-refining process intensification in catalytic conversion reactions, separations and purifications of hydroxymethylfurfural (HMF) and furfural. *Chem. Eng. J.* **2022**, *429*, 132325. [CrossRef]
8. Quiroz, N.R.; Norton, A.M.; Nguyen, H.; Vasileiadou, E.; Vlachos, D.G. Homogeneous metal salt solutions for biomass upgrading and other select organic reactions. *ACS Catal.* **2019**, *9*, 9923–9952. [CrossRef]
9. Asim, A.M.; Uroos, M.; Naz, S.; Sultan, M.; Griffin, G.; Muhammad, N.; Khan, A.S. Acidic ionic liquids: Promising and cost-effective solvents for processing of lignocellulosic biomass. *J. Mol. Liq.* **2019**, *287*, 110943. [CrossRef]
10. Otomo, R.; Yokoi, T.; Kondo, J.N.; Tatsumi, T. Dealuminated Beta zeolite as effective bifunctional catalyst for direct transformation of glucose to 5-hydroxymethylfurfural. *Appl. Catal. A-Gen.* **2014**, *470*, 318–326. [CrossRef]
11. Liu, J.; Song, Y.; Zhuang, X.; Zhang, M.; Ma, L. Simplified preparation of a graphene-co-shelled Ni/NiO@C nano-catalyst and its application in the N-dimethylation synthesis of amines under mild conditions. *Green Chem.* **2021**, *23*, 4604–4617. [CrossRef]

12. Tang, H.; Li, N.; Li, G.; Wang, W.; Wang, A.; Cong, Y.; Wang, X. Dehydration of carbohydrates to 5-hydroxymethylfurfural over lignosulfonate-based acidic resin. *ACS Sustain. Chem. Eng.* **2018**, *6*, 5645–5652. [[CrossRef](#)]
13. Wang, S.; Eberhardt, T.L.; Pan, H. Efficient dehydration of fructose into 5-HMF using a weakly-acidic catalyst prepared from a lignin-derived mesoporous carbon. *Fuel* **2022**, *316*, 123255. [[CrossRef](#)]
14. Choudhary, V.; Mushrif, S.H.; Ho, C.; Anderko, A.; Nikolakis, V.; Marinkovic, N.S.; Frenkel, A.I.; Sandler, S.I.; Vlachos, D.G. Insights into the interplay of Lewis and Brønsted acid catalysts in glucose and fructose conversion to 5-(hydroxymethyl) furfural and levulinic acid in aqueous media. *J. Am. Chem. Soc.* **2013**, *135*, 3997–4006. [[CrossRef](#)]
15. Yang, H.; Guo, Q.; Yang, P.; Liu, X.; Wang, Y. Synthesis of hierarchical Sn-Beta zeolite and its catalytic performance in glucose conversion. *Catal. Today* **2021**, *367*, 117–123. [[CrossRef](#)]
16. Xing, X.; Guan, Y.; Zhang, L.; Shi, X.; Wu, H.; Gao, H.; Xu, S. Efficient formation of 5-hydroxymethylfurfural from glucose through H-β zeolite catalyst in the recyclable water-tetrahydrofuran biphasic system. *Catal. Today* **2022**, *404*, 229–236. [[CrossRef](#)]
17. Liu, Y.; Ding, G.; Wang, H.; Li, X.; Zhang, J.; Zhu, Y.; Yang, Y.; Li, Y. Highly selective glucose isomerization by HY zeolite in gamma-butyrolactone/H<sub>2</sub>O system over fixed bed reactor. *Catal. Commun.* **2021**, *156*, 106324. [[CrossRef](#)]
18. Xu, S.; Zhang, L.; Xiao, K.; Xia, H. Isomerization of glucose into fructose by environmentally friendly Fe/β zeolite catalysts. *Carbohydr. Res.* **2017**, *446*, 48–51. [[CrossRef](#)]
19. Xu, S.; Pan, D.; Hu, F.; Wu, Y.; Wang, H.; Chen, Y.; Yuan, H.; Gao, L.; Xiao, G. Highly efficient Cr/β zeolite catalyst for conversion of carbohydrates into 5-hydroxymethylfurfural: Characterization and performance. *Fuel Process. Technol.* **2019**, *190*, 38–46. [[CrossRef](#)]
20. Xia, H.; Hu, H.; Xu, S.; Xiao, K.; Zuo, S. Catalytic conversion of glucose to 5-hydroxymethylfurfural over Fe/β zeolites with extra-framework isolated Fe species in a biphasic reaction system. *Biomass Bioenerg.* **2018**, *108*, 426–432. [[CrossRef](#)]
21. Yi, F.; Chen, H.; Huang, L.; Hu, C.; Wang, J.; Li, T.; Wang, H.; Tao, Z.; Yang, Y.; Li, Y. Effects of the acidity and shape selectivity of dealuminated zeolite beta on butene transformations. *Fuel* **2021**, *300*, 120694. [[CrossRef](#)]
22. Wang, Y.; Otomo, R.; Tatsumi, T.; Yokoi, T. Dealumination of organic structure-directing agent (OSDA) free beta zeolite for enhancing its catalytic performance in n-hexane cracking. *Micropor. Mesopor. Mat.* **2016**, *220*, 275–281. [[CrossRef](#)]
23. Wang, W.N.; Zhang, W.; Chen, Y.L.; Wen, X.D.; Li, H.; Yuan, D.L.; Guo, Q.X.; Ren, S.Y.; Pang, X.M.; Shen, B.J. Mild-acid-assisted thermal or hydrothermal dealumination of zeolite beta, its regulation to Al distribution and catalytic cracking performance to hydrocarbons. *J. Catal.* **2018**, *362*, 94–105. [[CrossRef](#)]
24. Guo, X.; Li, J.; Wang, Y.; Rui, Z. Photothermocatalytic water splitting over Pt/ZnIn<sub>2</sub>S<sub>4</sub> for hydrogen production without external heat. *Catal. Today* **2022**, *402*, 210–219. [[CrossRef](#)]
25. Widayatno, W.B.; Guan, G.; Rizkiana, J.; Yang, J.; Hao, X.; Tsutsumi, A.; Abudula, A. Upgrading of bio-oil from biomass pyrolysis over Cu-modified β-zeolite catalyst with high selectivity and stability. *Appl. Catal. B-Environ.* **2016**, *186*, 166–172. [[CrossRef](#)]
26. Hillen, L.; Degirmenci, V. Synthesis methods for the production of hierarchically mesoporous and microporous zeolites. *Rev. Adv. Sci. Eng.* **2015**, *4*, 147–162. [[CrossRef](#)]
27. Gao, X.; Bare, S.R.; Weckhuysen, B.M.; Wachs, I.E. In situ spectroscopic investigation of molecular structures of highly dispersed vanadium oxide on silica under various conditions. *J. Phys. Chem. B* **1998**, *102*, 10842–10852. [[CrossRef](#)]
28. Valerio, G.; Goursot, A.; Vetrivel, R.; Malkina, O.; Malkin, V.; Salahub, D. Calculation of <sup>29</sup>Si and <sup>27</sup>Al MAS NMR chemical shifts in zeolite-β using density functional theory: Correlation with lattice structure. *J. Am. Chem. Soc.* **1998**, *120*, 11426–11431. [[CrossRef](#)]
29. Oozeerally, R.; Pillier, J.; Kilic, E.; Thompson, P.B.; Walker, M.; Griffith, B.E.; Hanna, J.V.; Degirmenci, V. Gallium and tin exchanged Y zeolites for glucose isomerisation and 5-hydroxymethyl furfural production. *Appl. Catal. A-Gen.* **2020**, *605*, 117798. [[CrossRef](#)]
30. Wang, Y.; Dai, Y.N.; Wang, T.H.; Li, M.L.; Zhu, Y.; Zhang, L.P. Efficient conversion of xylose to furfural over modified zeolite in the recyclable water/n-butanol system. *Fuel Process. Technol.* **2022**, *237*, 107472. [[CrossRef](#)]
31. Xu, H.; Li, X.; Hu, W.; Lu, L.; Chen, J.; Zhu, Y.; Zhou, H.; Si, C. Recent advances on solid acid catalytic systems for production of 5-hydroxymethylfurfural from biomass derivatives. *Fuel Process. Technol.* **2022**, *234*, 107338. [[CrossRef](#)]
32. Swift, T.D.; Nguyen, H.; Erdman, Z.; Kruger, J.S.; Nikolakis, V.; Vlachos, D.G. Tandem Lewis acid/Brønsted acid-catalyzed conversion of carbohydrates to 5-hydroxymethylfurfural using zeolite beta. *J. Catal.* **2016**, *333*, 149–161. [[CrossRef](#)]
33. Zhang, L.; Xi, G.; Zhang, J.; Yu, H.; Wang, X. Efficient catalytic system for the direct transformation of lignocellulosic biomass to furfural and 5-hydroxymethylfurfural. *Bioresour. Technol.* **2017**, *224*, 656–661. [[CrossRef](#)]
34. Zhao, J.; Zhou, C.; He, C.; Dai, Y.; Jia, X.; Yang, Y. Efficient dehydration of fructose to 5-hydroxymethylfurfural over sulfonated carbon sphere solid acid catalysts. *Catal. Today* **2016**, *264*, 123–130. [[CrossRef](#)]
35. Shi, N.; Liu, Q.; Wang, T.; Zhang, Q.; Tu, J.; Ma, L. Conversion of cellulose to 5-hydroxymethylfurfural in water-tetrahydrofuran and byproducts identification. *Chin. J. Chem. Phys.* **2015**, *27*, 711. [[CrossRef](#)]
36. Morais, A.R.C.; Bogel-Lukasik, R. Highly efficient and selective CO<sup>2-</sup> adjunctive dehydration of xylose to furfural in aqueous media with THF. *Green Chem.* **2016**, *18*, 2331–2334. [[CrossRef](#)]
37. Li, H.; Deng, A.; Ren, J.; Liu, C.; Wang, W.; Peng, F.; Sun, R. A modified biphasic system for the dehydration of d-xylose into furfural using SO<sub>4</sub><sup>2-</sup>/TiO<sub>2</sub>-ZrO<sub>2</sub>/La<sup>3+</sup> as a solid catalyst. *Catal. Today* **2014**, *234*, 251–256. [[CrossRef](#)]
38. Zhu, P.; Zhang, W.; Li, Q.; Xia, H. Visible-light-driven photocatalytic oxidation of 5-hydroxymethylfurfural to 2,5-furandicarboxylic acid over plasmonic Au/ZnO catalyst. *ACS Sustain. Chem. Eng.* **2022**, *10*, 8778–8787. [[CrossRef](#)]

39. Xia, H.; Xu, S.; Yan, X.; Zuo, S. High yield synthesis of 5-hydroxymethylfurfural from cellulose using  $\text{FePO}_4$  as the catalyst. *Fuel Process. Technol.* **2016**, *152*, 140–146. [[CrossRef](#)]
40. Carlini, C.; Patrono, P.; Galletti, A.M.R.; Sbrana, G. Heterogeneous catalysts based on vanadyl phosphate for fructose dehydration to 5-hydroxymethyl-2-furaldehyde. *Appl. Catal. A-Gen.* **2004**, *275*, 111–118. [[CrossRef](#)]

**Disclaimer/Publisher’s Note:** The statements, opinions and data contained in all publications are solely those of the individual author(s) and contributor(s) and not of MDPI and/or the editor(s). MDPI and/or the editor(s) disclaim responsibility for any injury to people or property resulting from any ideas, methods, instructions or products referred to in the content.